Dalton Transactions

ROYAL SOCIETY OF CHEMISTRY

PAPER

View Article Online
View Journal | View Issue

Cite this: *Dalton Trans.*, 2024, **53**, 9933

Thermodynamics of spin crossover in a bis(terpyridine) cobalt(II) complex featuring a thioether functionality†

Lúcio Ferraz Lobato, [a] Samuele Ciattini,[b] Angelo Gallo, [c] Rafael A. Allão Cassaro, [a] Lorenzo Sorace *[d] and Giordano Poneti *[a,e]

Received 26th February 2024,
Accepted 21st May 2024

DOI: 10.1039/d4dt00574k

rsc.li/dalton

In this contribution, a terpyridine-based ligand bearing a thioether functionality is used to prepare a new cobalt(II) spin crossover complex: $[Co(TerpyPhSMe)_2](PF_6)_2$ (**1**), where TerpyPhSMe is 4′-(4-methylthiophenyl)-2,2′:6′,2″-terpyridine. Its structure, determined by single crystal X-ray diffraction, reveals a *mer* coordination of the tridentate terpyridine ligands, leading to a tetragonally compressed octahedron. Intermolecular interactions in the crystal lattice freeze the complex in the high spin state in the solid state at all temperatures, as indicated by magnetometry and Electron Paramagnetic Resonance (EPR) spectra. When dissolved in acetonitrile, however, temperature dependent electronic, ^{1}H-NMR and EPR spectra highlight an entropy-driven spin crossover transition, whose thermodynamics parameters have been determined. This is the first report of a cobalt(II) SCO complex featuring a thioether group, allowing its implementation in chemically grown bistable monolayers and may open important perspectives for the use of such systems in molecular spintronics.

Introduction

Molecular materials with externally controllable physicochemical properties[1] are appealing candidates for sensors,[2] mechanical actuators,[3] units of storage[4] or treatment[5,6] of digital data. Complexes exhibiting Spin Crossover (SCO) are the most widely investigated class of switchable materials, featuring a transition between low spin and high spin electronic configurations, which is triggered by application of heat, pressure, magnetic field and other stimula.[7–9] Albeit being mostly found for pseudo-octahedral iron(II) complexes,[10] SCO has been observed also in coordination compounds based on different metal ions,[11–13] being cobalt(II) one of them.[11,14–17] Compared to iron(II) systems, cobalt(II) complexes are known to display more gradual entropy-driven SCO transitions.[18] More recently, they attracted attention for their ability to show thermal hysteretic SCO behaviour[19–21] and the possibility to act on their electronic state by electrochemical stimuli.[19]

Deposition of switchable molecular materials on solid surfaces in a controlled and reproducible manner is a mandatory step for their implementation in devices. Moreover, it offers a potential way to control their electronic state externally using physical properties of the supporting layer.[22] Indeed, the thioether,[23,24] thioacetyl,[25–27] or thiol[28–30] functional groups have been frequently used, in the past, to functionalize magnetic molecular materials in order to graft them on top of noble metal surfaces. In this respect, due to its ability to bind transition metal ions and the ample possibilities of functionalization, the 2,2′:6′,2″-terpyridine (tpy) molecular scaffold has proven to be a powerful building block for the development of discrete or supramolecular systems[31–33] with potential gas absorption, photovoltaic, luminescent and magnetic applications.[34–36] The 4′-position of the central pyridine ring is the most frequently encountered position for the derivatization of the terpyridine motif, yielding divergent molecular synthons for the preparation of coordination polymers.[33] Furthermore, terpyridine-based ligands are the most frequently reported in literature to provide cobalt(II) SCO systems.[11,17,37] By exploiting this approach, a complex where the cobalt(II) ion is coordinated by two terpyridine molecules functionalized in their 4′-position with a carboxylic acid

[a]*Instituto de Química, Universidade Federal do Rio de Janeiro, Rio de Janeiro, RJ, 21941-909, Brazil*
[b]*Interdepartmental Center for Crystallography (CRIST), University of Florence, Via della Lastruccia 3–13, 50019 Sesto Fiorentino, Italy*
[c]*Department of Chemistry, University of Turin, Via Pietro Giuria 7, 10125 Torino, Italy*
[d]*Department of Chemistry "U. Schiff" and INSTM Research Unit, University of Florence, Via della Lastruccia 3–13, 50019 Sesto Fiorentino, Italy. E-mail: lorenzo.sorace@unifi.it*
[e]*Dipartimento di Scienze Ecologiche e Biologiche, Università degli Studi della Tuscia, Largo dell'Università, 01100 Viterbo, Italy. E-mail: giordano.poneti@unitus.it*

†Electronic supplementary information (ESI) available: Experimental details, mass spectra of **1**, additional crystallographic information and spectroscopic data. CCDC 2335192 for **1**. For ESI and crystallographic data in CIF or other electronic format see DOI: https://doi.org/10.1039/d4dt00574k

recently revealed the persistence of SCO in a self-assembled monolayer on top of a silver surface.[38] This is the only example, up to date, of a chemisorbed self assembled monolayer of a SCO complex, clearly evidencing the need to search for other potential candidates.

With this aim, we have here used the 4′ position to functionalize the terpyridine scaffold with a thioether functional group, separated from the terpyridine motif by a phenyl ring, to prepare the 4′-(4-methylthiophenyl)-2,2′:6′,2″-terpyridine ligand (***TerpyPhSMe*** hereafter – Scheme 1). The ***TerpyPhSMe*** ligand has been previously employed to prepare coordination compounds with different metal ions (ruthenium(II),[39–41] iridium(III),[42] zinc(II)[43,44] and copper(II)[45]), but to the best of our knowledge, its potential for the preparation of switchable paramagnetic complexes is still unexplored.

The obtained ligand has been used to prepare a new cobalt-based complex, $[Co(TerpyPhSMe)_2](PF_6)_2$ (**1**): its structure has been determined by single-crystal X-ray diffraction and its magnetic behaviour in the solid state has been evaluated with magnetometry and electron paramagnetic resonance. In solution, its SCO behaviour has been evaluated with temperature dependent electronic spectroscopy and nuclear (^{1}H NMR) and electron (EPR) magnetic resonances.

Results and discussion

Synthesis

All manipulations were performed under aerobic conditions using materials as received. $CoCl_2{\cdot}6H_2O$, 2-acetylpyridine, 4-methylthiobenzaldehyde and potassium hexafluorophosphate were purchased from Aldrich and used as received. The 4′-(4-methylthiophenyl)-2,2′:6′,2″-terpyridine ligand (**TerpyPhSMe**) was synthesized according to a previously reported procedure.[39] Compound **1** has been prepared by reacting a methanolic solution of $CoCl_2{\cdot}6H_2O$ (0.133 g, 0.56 mmol) with a stirring methanol suspension of ***TerpyPhSMe*** (0.452 g, 1.27 mmol) and left to react at room temperature for 4 hours. After this, the solution was filtrated to eliminate any undissolved, unreacted material, and an aqueous solution of KPF_6 (0.207 g, 1.125 mmol) was added to the filtrate, causing the immediate separation of an orange precipitate. The obtained microcrystalline powder was subsequently recrystallized from a mixture of acetone and water. Mass spectrometry (Fig. S1†) and elemental analysis confirmed the expected structure of **1**. Yield: 86%. Anal. Calcd for $C_{44}H_{34}CoF_{12}N_6P_2S_2$: C, 49.87; H, 3.23; N, 7.93. Found: C, 50.06; H, 3.17; N, 7.62%. Selected IR data (cm^{-1}): 1599(m), 1479(w), 1419(w), 1248(w), 1079(w), 1017(w), 828(s), 650(w), 552(m), 503(w). ^{1}H NMR (600.17 MHz, CD_3CN) at 298 K δ (ppm): 92.36 (4H, s, 1), 54.35 (4H, s, 4), 43.6 (4H, s, 5), 32.27 (4H, s, 2), 13.77 (4H, s, 3), 9.14 (4H, s, 6), 9.09 (4H, s, 7), 3.55 (6H, s, 8).

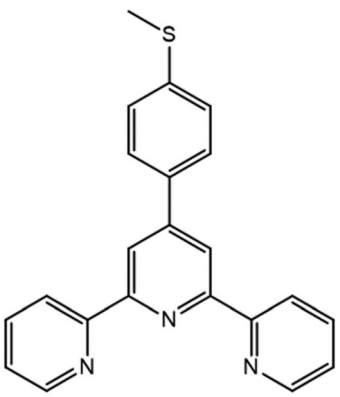

TerpyPhSMe ligand

Scheme 1

Solid state behaviour

Structural analysis. Single crystals of **1** suitable for X-ray diffractometry were grown from slow evaporation of a 50 : 50 acetone/water solution at room temperature. The crystal structure of **1** has been determined at 99 K and its asymmetric unit is shown in Fig. 1. Details of the data collection and structure refinement are reported in Table S1.† Compound **1** crystallizes in the $P2_1/c$ space group with 4 molecules per unit cell. The cobalt(II) ion is coordinated by the two terpyridine ligands in the classical bis-meridional fashion. The average Co–N bond length is 2.1285 Å, and the coordination environment can be described as an axially compressed octahedron, with Co–N2 and Co–N5 bond lengths being about 0.1 Å shorter than the average of the other four ones (see Table 1 selected bond lengths and angles). This is consistent with what previously observed for the high spin isomer of $[Co(tpy\text{-}R)]^{2+}$ cations.[16,20,21,46] In order to quantify the degree of distortion from ideal octahedral coordination of cobalt(II), Σ and ζ parameters were calculated using the OctaDist software,[48] and Continuous Shape Measure analysis (CShM) was carried out using the SHAPE software.[49] The ζ parameter describes the dispersion among the distances of the first coordination sphere ($\zeta = \sum_{i=1}^{6} |d_i - d_{mean}|$ where d_i and d_{mean} are Co–N bond lengths and average bond length, respectively), while Σ measures the deviation of the twelve *cis*-N–Co–N angles from 90° ($\Sigma = \sum_{i=1}^{12} |90 - \varphi|$ both are expected to be zero for a perfect octahedron). The obtained values of ζ = 0.25, Σ = 130.9 and CShM = 4.68 (see Table S2† for details) indicate that the octahedral coordination environment of cobalt(II) is significantly distorted. However, the ζ = 0.25 value obtained is in the expected range for high spin systems, while typically higher values are found for low-spin systems, due to Jahn–Teller distortions.[16] Therefore, all of these structural parameters indicate that in the single crystal phase of **1**, the cobalt(II) ion displays a high spin configuration at 99 K.

In the case of **1**, intermolecular π···π interactions are observed between pyridyl rings containing N4 and N6 and between pyridyl ring containing N4 and the phenyl ring of methylthiophenyl moiety of ***TerpyPhSMe*** ligand. Each molecule of the complex interacts with other three adjacent mole-

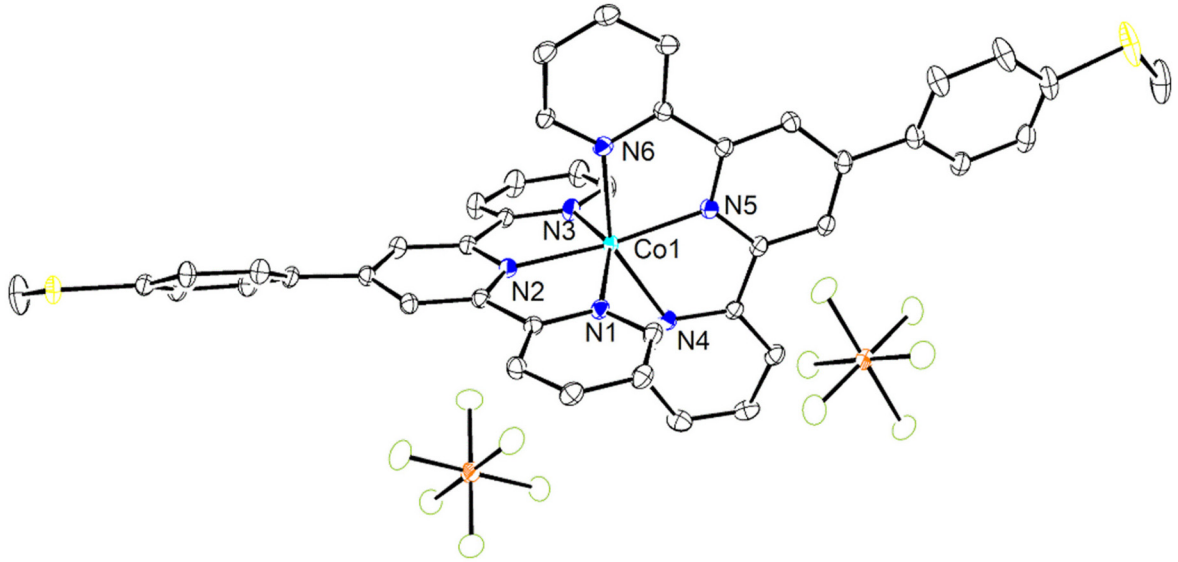

Fig. 1 ORTEP view of the asymmetric unit of **1** with the displacement ellipsoids drawn at 50% of probability. Hydrogen atoms have been omitted for clarity. Colour code: cobalt(II) ion (cyan), carbon (black), nitrogen (blue), sulphur (yellow), phosphorous (orange) and fluorine atoms (light green).

Table 1 Selected bond lengths and bond angles for **1**

Bond lengths (Å)			
Co1–N1	2.1765(18)	Co1–N4	2.1637(19)
Co1–N2	2.0699(18)	Co1–N5	2.0624(18)
Co1–N3	2.1573(19)	Co1–N6	2.1415(18)
Bond angles (°)			
N2–Co1–N1	75.21(7)	N2–Co1–N6	112.12(7)
N3–Co1–N1	149.39(7)	N3–Co1–N4	96.26(7)
N4–Co1–N1	95.93(7)	N5–Co1–N3	104.84(7)
N5–Co1–N1	105.31(7)	N6–Co1–N3	90.96(7)
N6–Co1–N1	91.54(7)	N5–Co1–N4	76.12(7)
N2–Co1–N3	75.61(7)	N6–Co1–N4	151.55(7)
N2–Co1–N4	96.33(7)	N5–Co1–N6	75.44(7)
N5–Co1–N2	172.44(7)		

cules leading to a two-dimensional network (Fig. S2†). The distances between centroids of pyridyl rings, and between centroids of pyridyl and phenyl rings are 3.718 and 4.004 Å, with the angle between planes being 15.4 and 17.8° and slippage of 1.614 and 1.244 Å, respectively. Other C–H···π and P–F···π interactions (not shown) were observed involving H3 and H43, with H···centroid distances of 2.76 and 2.99 Å, and C–H···centroid angles of 134 and 161°, respectively. The P2–F7···π (1 − *x*, −1/2 + *y*, 1/2 − z) intermolecular interaction involves the pyridyl moiety of **TerpyPhSMe** containing N5, with F7···centroid distance of 3.055 Å and P2–F7···centroid angle of 124.3°. These parameters are in the range found for π···π, C–H···π and P–F···π interactions in the literature.[52–55] In addition, PF_6^- anions interact with the complex through non-classical C–H···F hydrogen bonds (Fig. S3†).[56] The parameters found for the shortest H···F distances interactions are gathered in Table S3.† Many other weak intermolecular interactions with H···F distances spanning the range 2.45–2.54 Å were observed (not shown). These intermolecular interactions contribute to stabilization of crystal lattice and to the structural rigidity which locks **1** in the high spin state, in analogy to what was previously observed for other SCO complexes.[11,50,51]

EPR spectroscopy. The powder spectrum of **1** at different temperatures is reported in Fig. 2.

At low temperature the spectrum shows the typical features of a high spin cobalt(II) system, and can be interpreted by considering an effective $S = 1/2$ Spin Hamiltonian with largely anisotropic **g** tensor, resulting from the combined effect of distortions and spin–orbit coupling affecting the orbitally degenerate $^4T_{1g}$ state in purely octahedral symmetry.

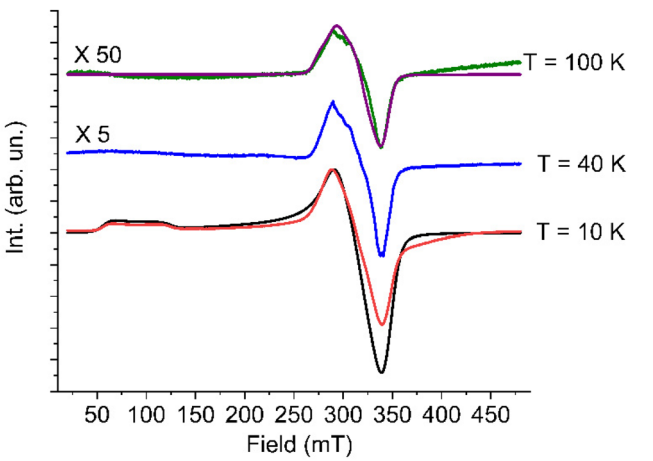

Fig. 2 Temperature dependence of the solid state EPR spectrum of **1** and best simulation for the $T = 10$ K spectrum (black line) and $T = 100$ K (purple line) obtained with models and parameters reported in the text. Spectra at 40 K and 100 K have been rescaled by factors reported on the left for a better appreciation.

In particular, the $g_z^{eff} > g_{x,y}^{eff}$ feature is consistent with a tetragonal compression of the octahedron, resulting in an orbital ground doublet, further split by spin–orbit coupling.[16] On increasing temperature the spectrum of the high spin species disappears as expected, due to the strong temperature dependence of the spin–lattice relaxation time of high-spin cobalt(II) in distorted octahedral environment. However, up to 100 K it remains a small trace of a broad and partially structured spectrum around g = 2.00, which we attribute to a fraction of low-spin cobalt(II) species.

A reliable simulation of the low temperature spectrum was obtained by using the following Spin Hamiltonian:[57]

$$\hat{H} = \mu_B B \cdot g_{eff} \cdot S_{eff} + S_{eff} \cdot A_{eff} \cdot I \quad (1)$$

where S_{eff} = 1/2 and I = 7/2, while A_{eff} accounts for the hyperfine interaction with magnetically active nucleus of ^{59}Co (100% natural abundance). The best simulation was obtained by using parameters $g_x^{eff} = 2.045 \pm 0.005$, $g_y^{eff} = 2.095 \pm 0.005$, $g_z^{eff} = 7.40 \pm 0.01$, $A_x^{eff} = A_y^{eff} = 5.0 \pm 0.5 \times 10^{-3}$ cm^{-1}, $A_z^{eff} = 29.5 \pm 0.5 \times 10^{-3}$ cm^{-1}. Both the g_{eff} principal values and the hyperfine coupling parameters are in good agreement with previous reports on high-spin complexes featuring terpyridine-like ligands.[16] The spectrum at 100 K can be simulated by considering an S = 1/2 species with $g_{x,y} = 2.20 \pm 0.02$, $g_z = 2.01 \pm 0.01$ and hyperfine coupling to an I = 7/2 nucleus and $A_x = (9 \pm 1) \times 10^{-3}$ cm^{-1} $A_y = (3.0 \pm 0.5) \times 10^{-3}$ cm^{-1}, and $A_z = (2.5 \pm 0.5) \times 10^{-3}$ cm^{-1}.

The observed pattern of effective g values for the high-spin species cannot be analyzed in the framework of an S = 3/2 Spin Hamiltonian[58] and requires resorting to a description of the electronic structure of distorted octahedral cobalt(II) which explicitly takes into account the unquenched orbital angular momentum first proposed by Griffith:[59,60]

$$\hat{H} = -\frac{3}{2}\kappa\lambda\hat{L}\cdot\hat{S} + \mu_B B \cdot \left(g_e\hat{S} - \frac{3}{2}\kappa\hat{L}\right) + \Delta_{ax}\left[\hat{L}_z^2 - \frac{1}{3}L(L+1)\right] \quad (2)$$

here the orbital (L = 1) and spin (S = 3/2) angular momenta characterizing the ground $^4T_{1g}$ term of the octahedral cobalt(II) ion interact through spin–orbit coupling, as described by the first term of the Hamiltonian and the orbital-reduction parameter (κ) takes into account the covalence effect and the crystal field induced mixing of $^4T_{1g}(^4F)$ with $^4T_{1g}(^4P)$. The third term of this Hamiltonian represents the effect of an axial crystal field which splits the $^4T_{1g}$ orbital triplet in octahedral symmetry into an orbital singlet $^4A_{2g}$ and an orbital doublet (^4E_g). The observation of a $g_z^{eff} > g_{x,y}^{eff}$ pattern can only be explained with a negative Δ_{ax} value, resulting in a ^4E_g ground state. A very good reproduction of the observed effective g values could be obtained by using the parameters λ = −180 cm^{-1}; κ = 0.9; Δ_{ax} = −200 cm^{-1}, resulting in a g_z^{eff} = 7.426, $g_{x,y}^{eff}$ = 2.136.[60,61] The Spin Hamiltonian parameters of the minority species responsible for the 100 K and the 50 K spectra are on the contrary consistent with low-spin cobalt(II) species previously reported in literature.[16,62] This clearly points to the powder sample containing a fraction of low spin species, in contrast with the pure high spin observed in the single crystal by X-ray diffractometry. Indeed, the PXRD pattern collected on the sample (Fig. S4†) shows the presence of a second phase in addition to the high spin one consistent with the pattern calculated using the single crystal structure. The coexistence of two phases with different spin states in microcrystalline powder, even if the single crystal behaviour indicates a pure high-spin phase, has been reported earlier for cobalt(II) complexes.[62]

Magnetometry. The temperature dependence of the product of the molar magnetic susceptibility times the absolute temperature ($\chi_M T$) of **1** has been measured in the solid state and is reported in Fig. 3.

The $\chi_M T$ value at room temperature (2.35 emu K mol^{-1}) is on the lower end of what expected for an octahedrally distorted high spin Co(II) centre, characterized by a relevant orbital contribution.[60] On cooling, the $\chi_M T$ values lower steadily until about 150 K, then more steeply to reach 1.39 emu K mol^{-1} at 10.0 K. The observed values are consistent with those observed by EPR spectroscopy, and point to a high-spin cobalt(II) configuration for **1** in the whole investigated temperature range but with a fraction of low-spin cobalt(II) species. In line with the results from the crystallographic analysis, which evidenced a structural rigidity imposed by the intermolecular interactions, no spin crossover is observed in the whole investigated temperature range. The observed data could be reasonably reproduced by using for the high spin species the same set of parameters of the Griffith Hamiltonian (eqn (2)) which were used to interpret the low temperature EPR spectrum,[61] and assuming the powder sample to contain a 25% fraction of low-spin cobalt(II) with a temperature independent $\chi_M T$ value of 0.4 emu K mol^{-1}.

Thus, the combined investigation of solid state EPR spectrum and magnetometry unequivocally indicate that **1** maintains the high spin configuration down to low temperature, despite indicating the presence of a non-negligible amount of

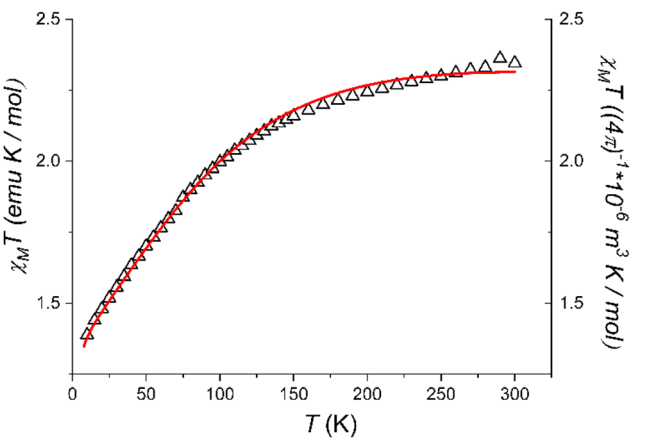

Fig. 3 Temperature evolution of the $\chi_M T$ product of **1** and simulated curve obtained using the parameter-free model reported in the text.

a temperature independent fraction of low-spin cobalt(II) species in the powder sample.

Solution behaviour

Electronic spectroscopy. Since solid state effects are known to critically affect the energy difference between the low- and high-spin state in SCO complexes,[21,47] an investigation of the SCO behaviour of **1** in solution has been performed. The temperature dependence of the electronic spectrum of an acetonitrile solution of **1** is reported in Fig. 4 (details on normalization and spectra before normalisation are reported in ESI, Fig. S5†).

All spectra are dominated by charge-transfer bands in the ultra-violet region, while the absorption band observed at 520 nm can be ascribed to a d–d transition of the low spin isomer of **1** ($^2A_1 \rightarrow {}^2T_1$, $^2T_2$), in analogy to what was previously inferred for the $[Co(tpy)_2]^{2+}$ cation.[63] Upon heating from 283 K to 343 K, an evolution of the electronic spectrum is observed, with the bands at 236 and 255 nm becoming more intense, and the other absorptions (280 and 520 nm) losing intensity, giving rise to an isosbestic point (here located at 300 nm due to the normalization condition of the spectra). Such behaviour is in line with an entropy-driven SCO equilibrium for **1**, with the high and low spin isomers coexisting in solution for every investigated temperature, due to the gradual nature of the transition in cobalt(II) SCO systems.

EPR spectroscopy. Given the indications of electronic spectroscopy of the dominant presence of low-spin cobalt(II) in solution, we performed EPR spectra in the same medium down to 10 K. The lowest temperature spectrum is reported in Fig. 5. A single broad line, partially anisotropic and hyperfine split is observed at field corresponding to $g = 2.10$. The spectrum was tentatively simulated with a Hamiltonian essentially equal to eqn (1), except that it now acts on a real $S = 1/2$ spin. The best simulation provided a set of parameters which is consistent with those of the low-spin minority species observed in the solid state sample and of other low-spin cobalt(II)-tpy complexes previously reported in literature:[16,62] $g_x = 2.015 \pm 0.005$, $g_y = 2.15 \pm 0.01$, $g_z = 2.20 \pm 0.01$, with $A_x = (2.2 \pm 0.2) \times 10^{-3}$ cm^{-1}, $A_y = (3.0 \pm 0.2) \times 10^{-3}$ cm^{-1}, and $A_z = (9.7 \pm 0.2) \times 10^{-3}$ cm^{-1}. Interestingly, no sign of the high spin species observed in the solid-state sample could be detected. On increasing temperature, in fact, the spectrum simply loses intensity, and disappears above the melting point of the solvent, thus not allowing to follow the SCO transition suggested by UV-Vis spectroscopy in fluid solution.

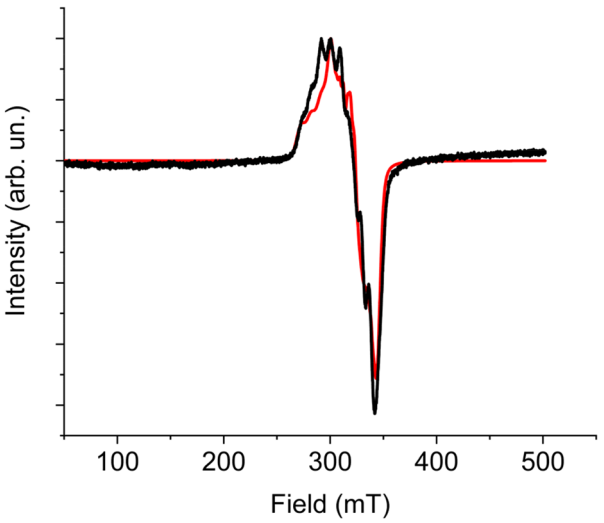

Fig. 5 X-Band EPR frozen solution spectrum of **1** recorded at 10 K and best simulation obtained using parameters reported in the text.

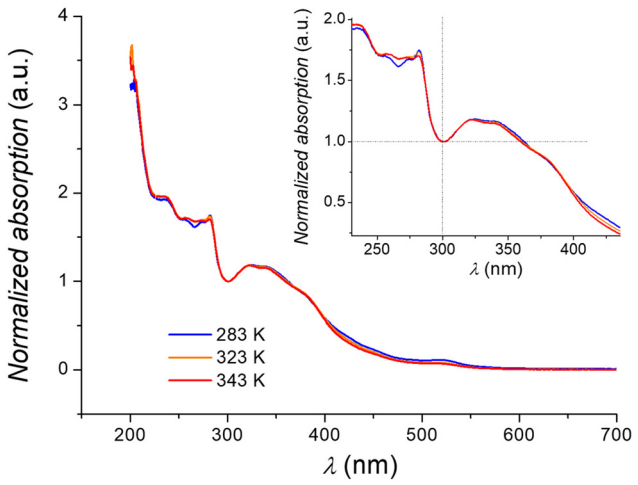

Fig. 4 Temperature dependence of the electronic spectrum of an acetonitrile solution of **1**. Inset: Zoom of the region around the isosbestic point at 300 nm.

^{1}H-NMR spectroscopy. NMR spectroscopy has been previously used to characterize spin equilibria in solution[64–70] as well as to foresee the use of SCO molecular materials as local thermometers.[71] Typically NMR spectroscopy is able to measure the magnetic moment of a sample in solution, either through the Evans method, or the paramagnetic shifts of its magnetically active nuclei. However, the Evans method is not much accurate for the determination of the thermodynamics parameters of the SCO in solution, since it requires a careful control of the concentration of the analyte's solution and has a limited accuracy.[70] For these reasons, we measured the temperature dependencies of the paramagnetic shifts in the ^{1}H-NMR spectra of **1** to follow its entropy-driven SCO equilibrium and determine the enthalpy ($\Delta H°$) and entropy ($\Delta S°$) variations associated to it. This approach allows us to fit several experimental observables with a single model at the same time, increasing the robustness of the obtained thermodynamics parameters. The dependencies of selected ^{1}H chemical shifts in ^{1}H-NMR spectrum of **1** in the 233–333 K range are shown in Fig. 6 (the complete ^{1}H-NMR spectrum of an acetonitrile-d_3 solution of **1** is reported in Fig. S6†).

The spectrum consists of 8 paramagnetically shifted signals over a 90 ppm frequency range, indicating the presence of a significant magnetic anisotropy in the susceptibility of **1**. The

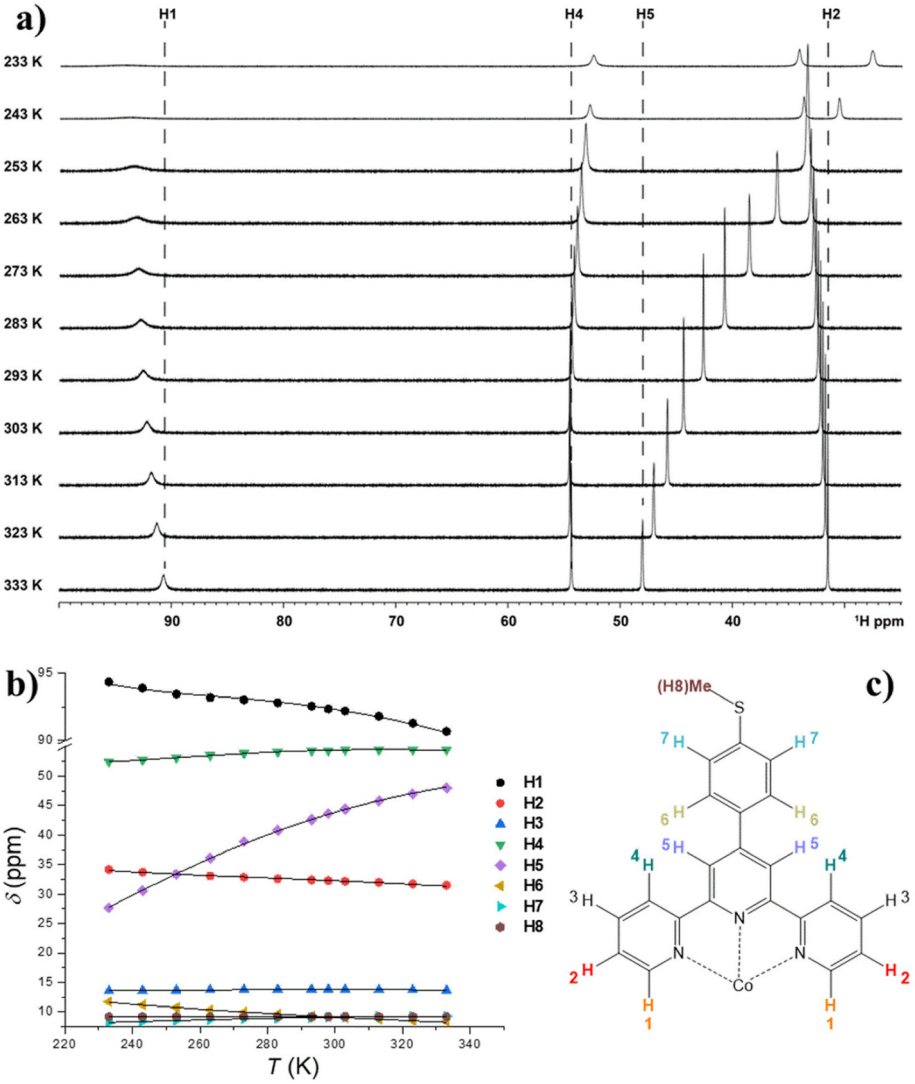

Fig. 6 Panel a: ^{1}H-NMR spectra of an acetonitrile-d_3 solution of **1** acquired at different temperatures (dashed lines indicates the chemical shifts assignment). Only selected resonances are shown for clarity. Panel b: Temperature dependence of the chemical shifts of every non-equivalent hydrogen of **1**. Lines are the best fitting curves, whose function and parameters are described in the text. Panel c: ^{1}H assignments for the ***TerpyPhSMe*** ligand in **1**.

spectral attribution has been carried out on the basis of the relative integrals of the various signals, the D_{2d} symmetry of the complex in solution and on a recent study of the ^{1}H-NMR spectrum of a structurally related system, $[Co(pytpy)_2](OTf)_2$, where pytpy is the 4′-(4‴-pyridyl)-2,2′:6′,2″-terpyridine ligand.[68]

It is evident that the chemical shift of H4 and H5 signals increases upon heating; this cannot be explained by the temperature dependence of the susceptibility of **1** in the solid state, which undergoes a monotonic decrease upon heating (see Fig. S7†). Rather, considering the outcome of the UV-Vis spectroscopy and solution EPR study, this behaviour can be interpreted assuming the onset of SCO behaviour in solution. Moreover, the continuous shifting of the peaks suggests that the high spin/low spin equilibrium is fast on our NMR time scale. Under this condition, the temperature dependence of the chemical shifts of the i^{th} signal can be fitted with eqn (3):[64,67]

$$\delta(T)_i = \frac{C_{LS,i}}{T} + \frac{(C_{HS,i} - C_{LS,i})}{T\left(e^{\left(\frac{\Delta H^\circ}{RT} - \frac{\Delta S^\circ}{R}\right)} + 1\right)} \quad (3)$$

where C_{LS} and C_{HS} are the Curie constants of the different peaks for the low and high spin isomers, respectively, and ΔH° and ΔS° are the enthalpy and entropy changes associated to the SCO equilibrium. Eqn (3) assumes that the signals of both isomers follow a Curie-like behaviour, and that the SCO transition profile is described by a Boltzmann distribution, with no intermolecular interactions. To reduce overparameterization, the chemical shift of each signal is supposed to arise

only from paramagnetic terms (contact and pseudocontact), ignoring its diamagnetic chemical shift, and the thermodynamic quantities are assumed to be temperature independent, even if this is not always the case for cobalt(II) SCO systems.[72] The fitting procedure was carried out for every peak simultaneously, and yielded values of the enthalpy and entropy change of the SCO equilibrium of 9.4(6) kJ mol^{-1} and 28(2) J K^{-1} mol^{-1}, respectively, in qualitative accord with previous reports of cobalt(II) SCO systems[73,74] (for a complete list of the best fitting parameters, see Table S4†). These quantities allow to estimate the transition temperature, $T_{1/2}$, featuring equivalent amounts of low and high spin isomers in solution, as 336(32) K. It must be stressed that attempts to fit the data including the diamagnetic contribution to each chemical shift led to the same thermodynamic values, but also to a huge increase in their uncertainties and were then not taken in consideration.

Conclusions

In this contribution, a terpyridine ligand functionalized with a thioether group, ***TerpyPhSMe***, has been used to prepare a new cobalt(II) complex designed as a potential candidate to observe spin crossover on chemically grafted monolayers. The molecular structure of complex **1** obtained by X-ray diffractometry shows that ***TerpyPhSMe*** ligand binds in the usual meridional fashion to yield a mononuclear complex featuring the thioether moieties uncoordinated. The axial compression of the octahedron, the analysis of the bond lengths and distortion of the first coordination sphere shows that **1** is a high spin complex in the solid state at 99 K. We attribute the absence of a spin conversion in the solid state to the intramolecular π–π interactions and non-classic C–H···F hydrogen bonds, which lock the molecule in the high spin isomeric form. Magnetometry and EPR confirms that **1** is a high spin complex in the solid state independently of the temperature but powder sample contains a fraction of low spin cobalt(II). After dissolution in acetonitrile, however, EPR indicates the sole presence of low spin cobalt(II) at low temperature, and temperature-dependent electronic spectra suggest the onset of an entropy-driven spin crossover equilibrium above room temperature, which is indeed confirmed by the temperature evolution of ^{1}H-NMR spectra. Fitting of the thermal dependencies of the chemical shifts using a Boltzmann distribution model allowed to extrapolate the thermodynamic quantities associated to it (ΔH° = 9.4(6) kJ mol^{-1} and ΔS° = 28(2) J K^{-1} mol^{-1}). This is extremely relevant in the perspective of using this complex to obtain switchable monolayers, where the solid state effects which lock the molecule in high spin state can be neglected.[30]

Conflicts of interest

There are no conflicts to declare.

Acknowledgements

GP and RAAC gratefully acknowledge FAPERJ for funding through grants E-26/202.912/2019, SEI-260003/001167/2020, E-26/010.000978/2019 and E-26/203.033/2018. RAAC acknowledges CAPES-PrInt (23079.241056/2023-17) for a fellowship. The authors thank Prof. Roberta Sessoli (Dipartimento di Chimica "*Ugo Schiff*", Università degli Studi di Firenze, Italy) and the Laboratório Multiusuário (Instituto de Física, Universidade Federal do Rio de Janeiro, Brazil) for providing access to the SQUID magnetometers. Dr Laura Chelazzi (*CRIST, University of Florence*) is acknowledged for single crystal X-ray diffraction data collection and processing, and Prof. Débora de Almeida Azevedo and Dr Thamara Andrade Barra (Instituto de Química, Universidade Federal do Rio de Janeiro) for the mass spectrometry analysis. Prof. Raffaele Saladino (Dipartimento di Scienze Ecologiche e Biologiche, University of Tuscia) is acknowledged for granting access to the electronic spectrometer. LS acknowledges the support of MUR through Progetto Dipartimenti di Eccellenza 2023–2027 (CUP B97G22000740001—DICUS 2.0).

References

1 O. Sato, *Nat. Chem.*, 2016, **8**, 644–656.
2 I.-R. Jeon, J. G. Park, C. R. Haney and T. D. Harris, *Chem. Sci.*, 2014, **5**, 2461–2465.
3 H. J. Shepherd, I. A. Gural'skiy, C. M. Quintero, S. Tricard, L. Salmon, G. Molnar and A. Bousseksou, *Nat. Commun.*, 2013, **4**, 2607.
4 T. Miyamachi, M. Gruber, V. Davesne, M. Bowen, S. Boukari, L. Joly, F. Scheurer, G. Rogez, T. K. Yamada, P. Ohresser, E. Beaurepaire and W. Wulfhekel, *Nat. Commun.*, 2012, **3**, 938.
5 A. Cornia and P. Seneor, *Nat. Mater.*, 2017, **16**, 505–506.
6 M. R. Wasielewski, M. D. E. Forbes, N. L. Frank, K. Kowalski, G. D. Scholes, J. Yuen-Zhou, M. A. Baldo, D. E. Freedman, R. H. Goldsmith, T. Goodson, M. L. Kirk, J. K. McCusker, J. P. Ogilvie, D. A. Shultz, S. Stoll and K. B. Whaley, *Nat. Rev. Chem.*, 2020, **4**, 490–504.
7 P. Gütlich and H. A. Goodwin, in *Spin Crossover in Transition Metal Compounds I*, ed. P. Gütlich and H. A. Goodwin, Springer, Berlin Heidelberg, 2004, vol. 233, pp. 1–47.
8 P. Gutlich, Y. Garcia and H. A. Goodwin, *Chem. Soc. Rev.*, 2000, **29**, 419–427.
9 *Spin-Crossover Materials: Properties and Applications*, ed. M. A. Halcrow, Wiley and Sons, 2013.
10 P. Gütlich, A. Hauser and H. Spiering, *Angew. Chem., Int. Ed. Engl.*, 1994, **33**, 2024–2054.
11 H. A. Goodwin, in *Spin Crossover in Transition Metal Compounds II*, ed. P. Gütlich and H. A. Goodwin, Springer, Berlin, Heidelberg, 2004, pp. 23–47.
12 Y. Garcia and P. Gütlich, in *Spin Crossover in Transition Metal Compounds II*, ed. P. Gütlich and H. A. Goodwin, Springer, Berlin, Heidelberg, 2004, pp. 49–62.

13 D. J. Harding, P. Harding and W. Phonsri, *Coord. Chem. Rev.*, 2016, **313**, 38–61.
14 O. Drath and C. Boskovic, *Coord. Chem. Rev.*, 2018, **375**, 256–266.
15 S. Hayami, M. Nakaya, H. Ohmagari, A. S. Alao, M. Nakamura, R. Ohtani, R. Yamaguchi, T. Kuroda-Sowa and J. K. Clegg, *Dalton Trans.*, 2015, **44**, 9345–9348.
16 I. Krivokapic, M. Zerara, M. L. Daku, A. Vargas, C. Enachescu, C. Ambrus, P. Tregenna-Piggott, N. Amstutz, E. Krausz and A. Hauser, *Coord. Chem. Rev.*, 2007, **251**, 364–378.
17 S. Hayami, Y. Komatsu, T. Shimizu, H. Kamihata and Y. H. Lee, *Coord. Chem. Rev.*, 2011, **255**, 1981–1990.
18 S. Brooker, P. G. Plieger, B. Moubaraki and K. S. Murray, *Angew. Chem., Int. Ed.*, 1999, **38**, 408–410.
19 M. G. Cowan, J. Olguín, S. Narayanaswamy, J. L. Tallon and S. Brooker, *J. Am. Chem. Soc.*, 2012, **134**, 2892–2894.
20 R. G. Miller, S. Narayanaswamy, J. L. Tallon and S. Brooker, *New J. Chem.*, 2014, **38**, 1932–1941.
21 D. Shao, L. Shi, F.-X. Shen, X.-Q. Wei, O. Sato and X.-Y. Wang, *Inorg. Chem.*, 2019, **58**, 11589–11598.
22 X. Zhang, T. Palamarciuc, J.-F. Letard, P. Rosa, E. V. Lozada, F. Torres, L. G. Rosa, B. Doudin and P. A. Dowben, *Chem. Commun.*, 2014, **50**, 2255–2257.
23 C. H. Chen, D. S. Krylov, S. M. Avdoshenko, F. Liu, L. Spree, R. Westerström, C. Bulbucan, M. Studniarek, J. Dreiser, A. U. B. Wolter, B. Büchner and A. A. Popov, *Nanoscale*, 2018, **10**, 11287–11292.
24 L. Zobbi, M. Mannini, M. Pacchioni, G. Chastanet, D. Bonacchi, C. Zanardi, R. Biagi, U. Del Pennino, D. Gatteschi, A. Cornia and R. Sessoli, *Chem. Commun.*, 2005, 1640–1642.
25 F. Pineider, M. Mannini, C. Danieli, L. Armelao, F. M. Piras, A. Magnani, A. Cornia and R. Sessoli, *J. Mater. Chem.*, 2010, **20**, 187–194.
26 L. Poggini, E. Tancini, C. Danieli, A. L. Sorrentino, G. Serrano, A. Lunghi, L. Malavolti, G. Cucinotta, A.-L. Barra, A. Juhin, M.-A. Arrio, W. Li, E. Otero, P. Ohresser, L. Joly, J. P. Kappler, F. Totti, P. Sainctavit, A. Caneschi, R. Sessoli, A. Cornia and M. Mannini, *Adv. Mater. Interfaces*, 2021, **8**, 2101182.
27 L. Poggini, A. Lunghi, A. Collauto, A. Barbon, L. Armelao, A. Magnani, A. Caneschi, L. Sorace and M. Mannini, *Nanoscale*, 2021, **13**, 7613–7621.
28 D. Gatteschi, A. Cornia, M. Mannini and R. Sessoli, *Inorg. Chem.*, 2009, **48**, 3408–3419.
29 M. Mannini, F. Pineider, P. Sainctavit, C. Danieli, E. Otero, C. Sciancalepore, A. M. Talarico, M. A. Arrio, A. Cornia, D. Gatteschi and R. Sessoli, *Nat. Mater.*, 2009, **8**, 194–197.
30 G. Poneti, L. Poggini, M. Mannini, B. Cortigiani, L. Sorace, E. Otero, P. Sainctavit, A. Magnani, R. Sessoli and A. Dei, *Chem. Sci.*, 2015, **6**, 2268–2274.
31 H. Hofmeier and U. S. Schubert, *Chem. Soc. Rev.*, 2004, **33**, 373–399.
32 E. C. Constable, *Chem. Soc. Rev.*, 2007, **36**, 246–253.
33 C. E. Housecroft, *CrystEngComm*, 2015, **17**, 7461–7468.
34 P. C. Mondal, V. Singh and M. Zharnikov, *Acc. Chem. Res.*, 2017, **50**, 2128–2138.
35 L. Fioravanti, L. Bellucci, L. Armelao, G. Bottaro, F. Marchetti, F. Pineider, G. Poneti, S. Samaritani and L. Labella, *Inorg. Chem.*, 2022, **61**, 265–278.
36 L. Bellucci, L. Fioravanti, L. Armelao, G. Bottaro, F. Marchetti, F. Pineider, G. Poneti, S. Samaritani and L. Labella, *Chem. – Eur. J.*, 2023, **29**, e202202823.
37 S. Brooker, *Chem. Soc. Rev.*, 2015, **44**, 2880–2892.
38 V. García-López, N. Giaconi, L. Poggini, J. Calbo, A. Juhin, B. Cortigiani, J. Herrero-Martín, E. Ortí, M. Mannini, M. Clemente-León and E. Coronado, *Adv. Funct. Mater.*, 2023, **33**, 2300351.
39 E. C. Constable, C. E. Housecroft, E. Medlycott, M. Neuburger, F. Reinders, S. Reymann and S. Schaffner, *Inorg. Chem. Commun.*, 2008, **11**, 518–520.
40 D. C. Wanniarachchi, M. J. Heeg and C. N. Verani, *Inorg. Chem.*, 2014, **53**, 3311–3319.
41 R. Dhiman, N. Singh, B. Ugale and C. M. Nagaraja, *RSC Adv.*, 2017, **7**, 39325–39333.
42 E. C. Constable, C. E. Housecroft, G. E. Schneider, J. A. Zampese, H. J. Bolink, A. Pertegás and C. Roldan-Carmona, *Dalton Trans.*, 2014, **43**, 4653–4667.
43 J. Jiang, J. Li, C. Liu, R. Liu, X. Liang, Y. Zhou, L. Pan, H. Chen and Z. Ma, *J. Biol. Inorg. Chem.*, 2020, **25**, 311–324.
44 J. Li, R. Liu, J. Jiang, X. Liang, L. Huang, G. Huang, H. Chen, L. Pan and Z. Ma, *Molecules*, 2019, **24**, 4519.
45 J. Li, H. Yan, Z. Wang, R. Liu, B. Luo, D. Yang, H. Chen, L. Pan and Z. Ma, *Dalton Trans.*, 2021, **50**, 8243–8257.
46 M. Nakaya, R. Ohtani, J. W. Shin, M. Nakamura, L. F. Lindoy and S. Hayami, *Dalton Trans.*, 2018, **47**, 13809–13814.
47 M. A. Halcrow, *Chem. Soc. Rev.*, 2011, **40**, 4119–4142.
48 R. Ketkaew, Y. Tantirungrotechai, P. Harding, G. Chastanet, P. Guionneau, M. Marchivie and D. J. Harding, *Dalton Trans.*, 2021, **50**, 1086–1096.
49 M. C. Llunell, D. Cirera, J. Alemany and P. Alvarez, *SHAPE: Program for the Stereochemical Analysis of Molecular Fragments by Means of Continuous Shape Measures and Associated Tools*, 2013.
50 N. Bridonneau, L. Rigamonti, G. Poneti, D. Pinkowicz, A. Forni and A. Cornia, *Dalton Trans.*, 2017, **46**, 4075–4085.
51 B. J. C. Vieira, V. da Gama, I. C. Santos, L. C. J. Pereira, N. A. G. Bandeira and J. C. Waerenborgh, *CrystEngComm*, 2018, **20**, 2465–2475.
52 C. Janiak, *J. Chem. Soc., Dalton Trans.*, 2000, 3885–3896.
53 M. Nishio, *CrystEngComm*, 2004, **6**, 130–158.
54 A. Di Santo, H. Pérez, G. A. Echeverría, O. E. Piro, R. A. Iglesias, R. E. Carbonio, A. Ben Altabef and D. M. Gil, *RSC Adv.*, 2018, **8**, 23891–23902.
55 P. Li, J. M. Maier, E. C. Vik, C. J. Yehl, B. E. Dial, A. E. Rickher, M. D. Smith, P. J. Pellechia and K. D. Shimizu, *Angew. Chem., Int. Ed.*, 2017, **56**, 7209–7212.
56 E. D'Oria and J. J. Novoa, *CrystEngComm*, 2008, **10**, 423–436.
57 S. Stoll and A. Schweiger, *J. Magn. Reson.*, 2006, **178**, 42–55.

58 A. V. Palii, D. V. Korchagin, E. A. Yureva, A. V. Akimov, E. Y. Misochko, G. V. Shilov, A. D. Talantsev, R. B. Morgunov, S. M. Aldoshin and B. S. Tsukerblat, *Inorg. Chem.*, 2016, **55**, 9696–9706.
59 J. S. Griffith, *The Theory of Transition-Metal Ions*, Cambridge University Press, Cambridge, 1961.
60 F. Lloret, M. Julve, J. Cano, R. Ruiz-García and E. Pardo, *Inorg. Chim. Acta*, 2008, **361**, 3432–3445.
61 N. F. Chilton, R. P. Anderson, L. D. Turner, A. Soncini and K. S. Murray, *J. Comput. Chem.*, 2013, **34**, 1164–1175.
62 S. Kremer, W. Henke and D. Reinen, *Inorg. Chem.*, 1982, **21**, 3013–3022.
63 C. Enachescu, I. Krivokapic, M. Zerara, J. A. Real, N. Amstutz and A. Hauser, *Inorg. Chim. Acta*, 2007, **360**, 3945–3950.
64 W. Klaeui, W. Eberspach and P. Guetlich, *Inorg. Chem.*, 1987, **26**, 3977–3982.
65 L. A. Yatsunyk and F. A. Walker, *Inorg. Chem.*, 2004, **43**, 757–777.
66 B. Weber and F. A. Walker, *Inorg. Chem.*, 2007, **46**, 6794–6803.
67 H.-J. Lin, D. Siretanu, D. A. Dickie, D. Subedi, J. J. Scepaniak, D. Mitcov, R. Clérac and J. M. Smith, *J. Am. Chem. Soc.*, 2014, **136**, 13326–13332.
68 A. A. Pavlov, G. L. Denisov, M. A. Kiskin, Y. V. Nelyubina and V. V. Novikov, *Inorg. Chem.*, 2017, **56**, 14759–14762.
69 S. E. Creutz and J. C. Peters, *Inorg. Chem.*, 2016, **55**, 3894–3906.
70 Y. Pankratova, D. Aleshin, I. Nikovskiy, V. Novikov and Y. Nelyubina, *Inorg. Chem.*, 2020, **59**, 7700–7709.
71 A. E. Thorarinsdottir, A. I. Gaudette and T. D. Harris, *Chem. Sci.*, 2017, **8**, 2448–2456.
72 M. Zerara and A. Hauser, *ChemPhysChem*, 2004, **5**, 395–399.
73 M. G. Simmons and L. J. Wilson, *Inorg. Chem.*, 1977, **16**, 126–130.
74 J. K. Beattie, R. A. Binstead, M. T. Kelso, P. Del Favero, T. G. Dewey and D. H. Turner, *Inorg. Chim. Acta*, 1995, **235**, 245–251.